POTENTIAL CLIMATE CHANGE EFFECTS ON GREAT LAKES HYDRODYNAMICS AND WATER QUALITY

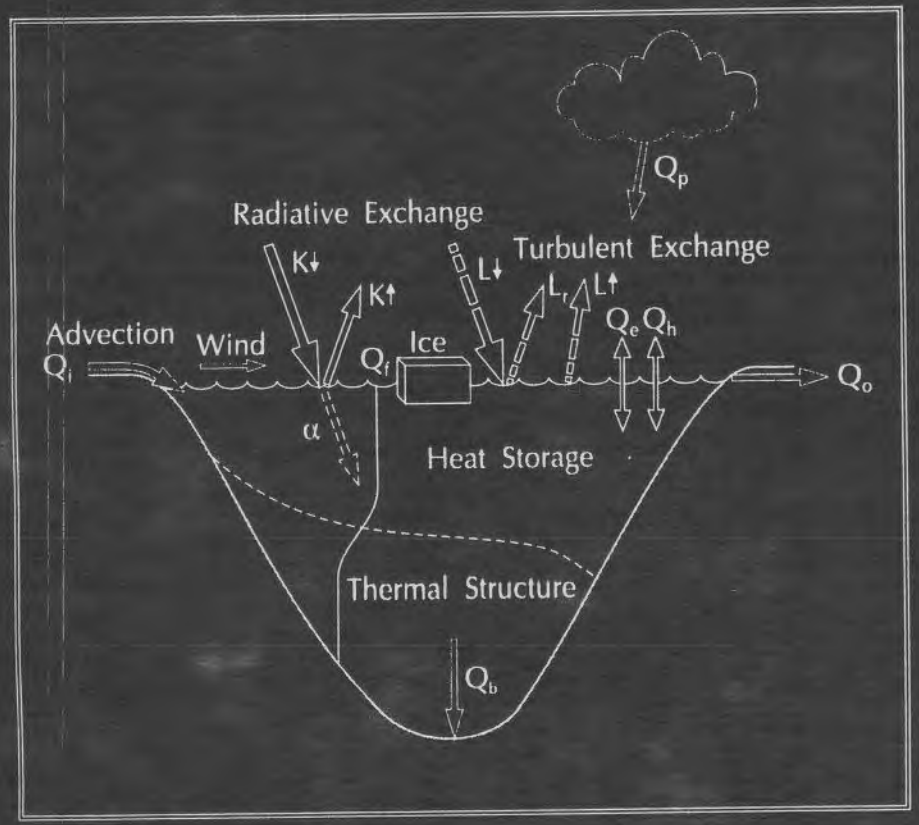

EDITED BY DAVID C.L. LAM AND WILLIAM M. SCHERTZER

ASCE

Chapter 3
LAKE THERMODYNAMICS

Michael J. McCormick[1] and David C. L. Lam[2]

ABSTRACT : *Vertical heat transfer is the most dominant process in lake thermodynamics, strongly affecting vertical mass and energy distributions and the lake ecosystem. Many theoretical studies (Section 3.1) on thermal structure forecasting or mixed layer (ML) modeling have used the one-dimensional approach with various formulations (Sections 3.2 and 3.6). By comparing predicted results from four ML models for three GCM scenarios (Section 3.3) it was found that the models were useful, provided that they can solve the horizontal variabilities (lakewide vs. coastal) as well as the different temporal scales (climate effects vs. natural basin oscillations). Only when such theoretical and practical considerations are made, one would look carefully into possible climate change effects. As an example, in Section 3.4, application of the Garwood Model (1977) to Lake Michigan under a potential doubling of CO_2 shows pronounced changes in both the annual temperature cycle and heat content with the possibility for permanent stratification under some scenarios. This is not a climate change forecast but rather it documents the sensitivity of the lake's thermal structure to low frequency changes in the net surface heat flux that are often predicted by GCM's.*

3.1 INTRODUCTION

The vertical transport of heat at the ocean/lake surface is important if large temperature differences are to be avoided. For example, Ivanoff (1977) calculates that for a sunny summer midday, typical for the Western Mediterranean, the heating rate of the top cm of the ocean surface would approach 10.2 $^{\circ}C \cdot h^{-1}$. Although heating rates this high are not seen large gradients of nearly 5 $^{\circ}$C have been observed between 2-m and 4-

[1] NOAA, Great Lakes Environmental Research Laboratory, 2205 Commonwealth Blvd., Ann Arbor, MI, 48105. E-mail : mccormick@glerl.noaa.gov
[2] National Water Research Institute, Environment Canada, 867 Lakeshore Road, P.O. Box 5050, Burlington, Ontario L7R 4A6 Canada. E-Mail : David.Lam@CCIW.ca

cm below the ocean surface (Ramp et al., 1991). This illustrates the importance of understanding the response of large water bodies to forces resulting from heating and cooling and those due to wind stress at the water surface.

Thermal structure forecasting or mixed layer (ML) modeling has sustained attention over the past five decades because the same processes that govern thermocline development also controls the vertical transfer of mass and energy. Figure 3-1 depicts an idealized temperature profile which identifies the surface mixed layer and thermocline region.

Specific thermal structure forecasting applications include predicting the density field for circulation models, and estimating the evolution and timing of the thermal structure for ecological studies. Uncertainties still exist in understanding thermal structure with even one-dimensional models, yet there are certain applications, such as some climatology studies whereby one-dimensional models have outperformed three-dimensional simulations. Regardless of whether the vertical mixing mechanism is embedded in a three-dimensional model or used alone the physics of mixing is the same. The application skill of models based upon vertical mixing alone is dependent upon how well the one-dimensional assumptions hold over the time scales of interest. Therefore, for simplicity sake we will focus on one-dimensional vertical mixing only.

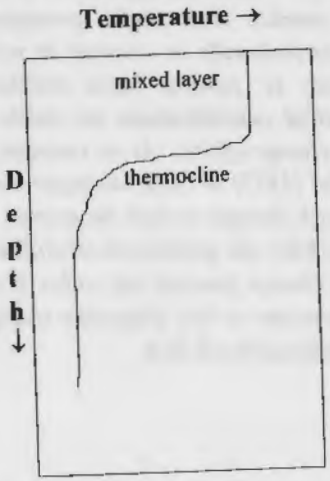

Figure 3-1. *Idealized temperature profile showing mixed layer and thermocline regions.*

The critical assumption that allows for one-dimensional treatment is that the local temperature profile is governed by local forces. Then in principle if the surface wind stress, initial temperature profile and surface fluxes are known, then too is the resulting thermal structure. However, serious prediction errors can result by ignoring advective effects. For example, De Szoeke (1980) considered an idealized case of horizontally uniform temperatures in the open ocean and demonstrated that the persistence of even a weak curl in the wind stress was sufficient to produce fronts and upwelling and downwelling zones. De Ruijter (1983) showed how a uniform wind field but nonuniform in space surface heat flux could produce similar effects Consequently, the ML depths in these areas would be poorly estimated by a strictly one-dimensional treatment. Here the horizontal transport of heat is too major a component of the local thermal budget to be ignored. Similar conclusions apply to large lakes.

In the Great Lakes region storm cycles can be expected every two to seven days (Oort and Taylor, 1969) and in consideration of storm size, basin areas, and coastal effects marked horizontal gradients in wind stress often result. When coupled with rotational effects complex circulation patterns occur with coastal jets, upwellings, downwellings, and rotational waves (e.g., Bennett, 1978; Boyce, 1974; Mortimer 1974). Hence, regions subject to large-scale vertical motions, such as coastal areas, are often poorly approximated by a one-dimensional model. Because of the problem's nonlinear nature even fully three-dimensional efforts have met with limited success in simulating the nearshore circulation and density field (Allender and Saylor, 1979; Bennett, 1977; Simons, 1976). Yet the one-dimensional approach can still be a useful tool if: (1) predictions are made far enough removed from coastal influences or equivalently in areas of minimum thermocline tilt or (2) predictions are made over long enough time periods so as to average out episodic events like upwellings and downwellings.

Before applying a model the relevant time and space scales that pertain to the water body of interest must be known. The theoretical width of the coastal boundary layer is proportional to r, the internal Rossby radius of deformation and is equal to $C \cdot f^{-1}$ where, C is the phase speed of a long internal wave propagating along the thermocline and f is the Coriolis parameter. For the Great Lakes this suggests a coastal zone width on the order of 2r or 10 km (Csanady, 1975). Observations in Lake Huron (Murthy and Dunbar, 1981), in Lake Ontario (Csanady, 1972), and in Lake Michigan (Ayers et al., 1958) suggest a boundary layer width consistent with this theory. For lakes smaller than the Great Lakes where rotational effects are not important Spigel and Imberger (1980) classify the dominant time scales of mixed layer dynamics in terms of the basin's geometry, wind forcing, and seasonal stratification.

The important time scales under transient conditions are diurnal, inertial, spin-up, and viscous diffusion. Heating of surface waters by solar radiation and sea-breeze effects often have a marked diurnal signal and are evident in current meter spectra. The inertial, spin-up, and viscous diffusion scales reflect the time periods over which wind driven currents are expected to vary. They are linked together by the Ekman number and the inertial period (Mohammed-Zaki, 1980). The Ekman number, $E = 2K_v f^{-1} H^{-2}$, where K_v is the eddy viscosity and H is the basin depth, expresses the ratio of the turbulent viscous to inertial forces. The inertial period, $T_i = 2\pi f^{-1}$, is always important and equal to about 17 h at Great Lakes latitudes. T_i is the time required for a fluid particle to rotate 360° about the local vertical axis. The spin-up time, $T_s = T_i E^{-.5}$, and the viscous diffusion time, $T_d = T_i E^{-1}$, are the required times to accelerate the water column to geostrophic equilibrium with a surface stress, and to damp out these oscillations upon cessation of the wind, respectively. All of the Great Lakes except Lake Erie are deep and have small Ekman numbers and as a result have distinguishable circulation time scales. However, in Lake

Erie the Ekman number is near enough to unity that the different scales are difficult to separate and the inertial period becomes the dominant time scale.

3.2 MIXED LAYER MODELS

In general, there are four approaches to calculating thermal structure (Niiler and Kraus, 1977): 1) turbulence closure models, 2) deterministic solutions, 3) eddy diffusion models, and 4) integrated ML models. All attempt to describe the evolution of the temperature field either by direct solution or by a combination of parameterization and simplification of the momentum, thermal, and the turbulence kinetic energy (TKE) equations through physically based arguments on the mixing processes. The four approaches have evolved from their treatment of the Reynolds stresses.

First, turbulence closure models solve for the Reynolds stresses through higher-order turbulence terms. The resulting triple-correlation products require additional assumptions and coefficients that must be empirically defined in order to solve the model's equations. The Mellor and Yamada level 2.5 model (Mellor and Yamada, 1982) represents this approach and it will described later in greater detail.

Second, deterministic solutions calculate the Reynolds stresses directly and have been attempted by Deardorff (1970). This approach requires very fine spatial grids and high temporal resolution of the dependent variables and initial conditions, however, it is too time consuming to be of practical interest.

Third, the eddy diffusion or "K" models are based on the thermal energy equation and on the assumption that the Reynolds stresses can be expressed according to Fick's law,

$$\overline{w'T'} = -K_H \frac{\partial \overline{T}}{\partial z}, \qquad \overline{w'v'} = -K_m \frac{\partial \overline{V}}{\partial z}$$

where K_H is the eddy diffusivity, and K_m is the eddy viscosity. It is a bold assumption to assume a local relationship between mean scalar fields and eddy fluxes (Davis, 1983) because theoretical principles suggest that none exists (Batchelor and Townsend, 1956; Roberts, 1961). Nonetheless, this has been a popular approach since Munk and Anderson (1948) first used it to describe thermocline formation. However, this approach has been criticized on two accounts. The physical basis for K models stems from Taylor's (1931) work where the eddy transfer coefficient is formulated in terms of a Richardson Number stability parameter. The data set (Jacobsen, 1913) used in formulating the Richardson Number has been criticized by Woods (1977) as being too limited (i.e., data were taken from the Kattegat at eight levels separated by 2.5 m) and thus is too weak a foundation for developing models. The second objection is concerned with the lack of a meaningful scale dependence. For example, Hoeber (1972) noted in the tropical North Atlantic an order of magnitude increase in the eddy viscosity with a 1-m·s^{-1} increase in the wind speed. This sensitivity to environmental conditions limits confidence in vertical transport predictions. Although these criticisms are severe, the popularity of this approach remains and can still be useful provided care is taken to recognize K model limitations. For example, the K model approach has been used successfully in the simulation of water temperatures and thermal layer thickness in many stratified lakes (Walter et al., 1978; Lam and Schertzer, 1987; Simons, 1980; Henderson-Sellers, 1985 and 1988). While the theoretical limitation was that some coefficients in the K models were lake-dependent, i.e. requiring model calibration with observed data on a lake by lake basis, the results are such that the simulated results were uniformly well predicted for many years for the same lake (Lam and Schertzer, 1987). On the other hand, mixed layer models have the advantage of using so-called universal constants and have the advantage of lake independence. However, these generalized constants may generate results that fit well in one year but not another (Blumberg and DiToro, 1990). Thus, for more dependable simulation, the K models have been adapted readily to the investigation of lake thermal responses (Section 2.5.2) and water quality problems such as oxygen depletion and algal growth (Section 7.7). Also, a number of improvements on the K models have been proposed. Henderson-Sellers (1985) used an analytical representation of the neutral eddy diffusion coefficients to avoid the specification of current profiles. Others (Simons,1980; Meyer et al.,1994) incorporated some forms of energy formulation in the eddy diffusivity. In this way, the K model approach and the mixed layer approach are complementary rather than competitive to each other (Stefan and Ford, 1975). For the remaining part of this chapter, our discussions will be devoted to the discussions of mixed layer models because of their theoretical significance for the investigation of climatic effects in lakes.

The fourth type of thermocline model originated with Kraus and Turner (1967) and stems from assumptions based on observations of upper ocean structure. Discontinuities in temperature and dissolved components are observed across the air-sea interface and across the base of the ML. Within the surface ML these distributions are, however, relatively uniform and can be represented as bulk or integrated variables, behaving as if the upper layers are responding as a "slab" to the external forcing. This model type may be further subdivided into two classes based upon physical assumptions by which water is entrained and the ML deepens. They are turbulent erosion models (TEM) and dynamic instability models (DIM) (Cushman-Roison, 1981). Entrainment in the TEM approach is proportional to the wind energy input to the water column minus the work performed in overcoming the buoyancy forces at the base of the ML. This is the Kraus and Turner (1967) model type. The DIM approach parameterizes deepening events to occur when the mean flow becomes unstable. This approach originated with Pollard et al. (1973). Instabilities in the mean flow are assumed to be shear generated with inertial oscillations as the shear source.

Two ML models will be described along with the turbulence closure model. The first by Thompson (1976) is an example of a DIM type model and the second ML model is by Garwood (1977) and uses mixing mechanisms from both the TEM and DIM model types. The models will be referred to by the author's initials: "ML2.5" for the Mellor and Yamada (1982) model, "RT" for the Thompson (1976) model in reference to Rhines and Thompson (R.O.R.Y. Thompson, personal communication, 1987), and "RWG" for the Garwood (1977) model.

3.2.1 ML2.5 model

The ML2.5 model is based upon conservation of heat, momentum, and TKE in the vertical (with all overbars omitted, see 3. 6 Appendix , for a derivation of the basic theory)

$$\frac{\partial u}{\partial t} - fv = \frac{\partial}{\partial z}\left(K_m + \upsilon_m \frac{\partial u}{\partial z}\right) \quad (3\text{-}1)$$

$$\frac{\partial v}{\partial t} + fu = \frac{\partial}{\partial z}\left(K_m + \upsilon_m \frac{\partial v}{\partial z}\right) \quad (3\text{-}2)$$

$$\frac{\partial T}{\partial t} = \frac{\partial}{\partial z}\left(K_H + \upsilon_H \frac{\partial T}{\partial z}\right) + \frac{1}{\rho_0 C_P}\frac{\partial R}{\partial z} \quad (3\text{-}3)$$

$$\frac{\partial q}{\partial t} = \frac{\partial}{\partial z}\left(K_q \frac{\partial q}{\partial z}\right) + K_m\left[\left(\frac{\partial u}{\partial z}\right)^2 + \left(\frac{\partial v}{\partial z}\right)^2\right] + K_H \frac{g}{\rho_0}\frac{\partial \rho}{\partial z} - \frac{(2q)^{1.5}}{cl} \quad (3\text{-}4)$$

where

K_q is the eddy diffusion coefficient for TKE;
$\upsilon_{m,H}$ background K_m and K_H, respectively;
l turbulence length scale; and
c a constant which modifies l.

The boundary conditions are:

$$(K_m + \upsilon_m)\frac{\partial u}{\partial z}\bigg|_{z=0} = \frac{\tau^x}{\rho_0} \quad (3\text{-}5)$$

$$(K_m + \upsilon_m)\frac{\partial v}{\partial z}\bigg|_{z=0} = \frac{\tau^y}{\rho_0} \quad (3\text{-}6)$$

$$(K_H + \upsilon_H)\frac{\partial T}{\partial z}\bigg|_{z=0} = \frac{Q}{\rho_0 C_P} \quad (3\text{-}7)$$

$$(K_H + \upsilon_H)\frac{\partial T}{\partial z}\bigg|_{z=-H} = 0 \quad (3\text{-}8)$$

where

$\tau^{x,y}$ are the eastward and northward components of the wind stress vector τ, respectively, equal to $\rho_a C_d |W| W$;
ρ_a air density;
C_d stability dependent drag coefficient at 10 m;
W wind vector;
Q surface heat flux; and
H lake depth.

The eddy coefficients K_m , K_H, and K_q govern the mixing rates within the mixed layer. Ignorance of these processes has led to assuming K_q equal to K_m. K_m and K_H are calculated by

$$K_H = l(2q)^{0.5} S_H$$
$$K_m = l(2q)^{0.5} S_m \quad (3\text{-}9)$$

where S_m and S_H are stability dependent functions based upon a local Richardson Number.

The last remaining parameter, l, is specified according to the Blackadar boundary layer formula

$$l = \left(l_0^{-1} + (\kappa z)^{-1}\right)^{-1}$$
$$l_0 = \left(\gamma \int_{-h}^{0} |z|(2q)^{0.5} dz\right)\left[\int_{-h}^{0} (2q)^{0.5} dz\right]^{-1} \quad (3\text{-}10)$$

where κ is Von Karman's constant and is equal to 0.4. The constant γ is set at 0.2.

3.2.2 RWG model

The RWG model (Garwood, 1977) contains deepening mechanisms that are found in both the DIM and TEM model types. Garwood recognized the nonisotropic nature of turbulence and thus decomposed the TKE into horizontal and vertical components as described in Equations (3-11) through (3-14).

$$0 = m_3 u_*^3 - \left[\frac{(\Delta u)^2 + (\Delta v)^2}{2}\right]\frac{\partial h}{\partial} - m_2\left(2q - 3w'^2\right)(2q)^{0.5} - \frac{2}{3}\left(m_1(2q)^{1.5} + 2m_5 fhq\right) \quad (3\text{-}11)$$

$$0 = -\alpha g \frac{h}{2}\Delta T \frac{\partial h}{\partial} + \Phi + m_2\left(2q - 3w'^2\right)(2q)^{0.5} - \frac{1}{3}\left(m_1(2q)^{1.5} + 2m_5 fhq\right) \quad (3\text{-}12)$$

$$\Phi = -\frac{\alpha g h}{2\rho_0 C_P}[Q + R(0) + R(-h)] + \frac{\alpha g}{\rho_0 C_P}\int_{-h}^{0} R(z)dz \quad (3\text{-}13)$$

$$\alpha g h \Delta T \frac{\partial h}{\partial} = 2m_4 qw' \quad (3\text{-}14)$$

where

u_* is the friction velocity equal to $(\tau/\rho_0)^{0.5}$;

α volumetric expansion coefficient equal to $-\frac{1}{\rho_0}\frac{\partial \rho}{\partial T}$;

ΔT = T - T(-h);

Δu = u - u(-h), and Δv = v - v(-h).

If $\frac{\partial h}{\partial} < 0$, then the buoyancy flux is solely determined by Eq. (3-13) and all terms containing w' are set equal to zero (Martin, 1985). The velocity jump, Δu and Δv, can either be prescribed from data or, in large bodies of water such as the Great Lakes, determined from the calculated velocity structure such as that described later in the RT model. Both Martin (1985) and Garwood (1977) ignored the shear production term in Eq. (3-11) but it is retained here in order to better describe storm induced deepening events.

The constants m_1 and m_5 scale dissipation, m_2 scales the partitioning of TKE between the horizontal and vertical, m_3 scales the surface flux of TKE, and m_4 scales the energy flux at the ML base. Garwood (1977), Martin (1985), McCormick and Meadows (1988), and McCormick (1990) set $m_1=m_2=m_4=1.0$ and the optimal values for m_3 and m_5 were 4.5 and 4.6, respectively. These optimal values were found by Martin (1985) who applied the RWG model to North Pacific data and by McCormick and Meadows (1988) who applied it to Lake Erie.

3.2.3 RT model

The RT model (Thompson, 1976) is a DIM type model whereby ML deepening occurs whenever the velocity shear at the ML base is sufficiently large for entrainment to occur. If the total shear stress is assumed to be caused by inertial currents and a slab-like flow is also assumed then the momentum equations become

$$\frac{d(hu)}{dt} - fhv = \frac{\tau^x}{\rho_0} \qquad (3\text{-}15)$$

$$\frac{d(hv)}{dt} + fhu = \frac{\tau^y}{\rho_0}. \qquad (3\text{-}16)$$

Thermal heating is described by

$$\frac{dT}{dt} = \frac{Q + R(0) - R(-h)}{h\rho_0 C_p} \qquad -h \le z < 0 \qquad (3\text{-}17)$$

$$\frac{\partial T}{\partial} = \upsilon_H \frac{\partial^2 T}{\partial z^2} + \frac{1}{\rho_0 C_p}\frac{\partial R}{\partial z} \qquad z < -h. \qquad (3\text{-}18)$$

In Eqs. (3-15) - (3-17) the ML velocities are depth integrated over the ML, whereas below the ML the temperature structure is determined by passive heating and background

mixing (Eq. 3-18), with further modifications dependent upon the extent and frequency of ML depth excursions. These equations represent the Pollard et al. (1973) model. Thompson (1976) further assumed that the momentum be held to zero below the ML base. This assumption avoids the need to specify additional model parameterizations and is justified because it is the current shear not magnitude that controls deepening. Finally, the model equations are closed by assuming that the ML flow remains marginally stable. Thompson (1979) reformulated closure in terms of a Froude Number, F, and suggested it remain at unity throughout the ML

$$F = \frac{u^2 + v^2}{gh\Delta\rho/\rho_0} = 1 \qquad -h \le z < o \qquad (3\text{-}19)$$

where $\Delta\rho = \rho - \rho(-h)$.

3.3 MODEL COMPARISONS AND PERFORMANCE

Two of the models (RT and RWG) were used in Lake Erie simulations by McCormick and Meadows (1988) while Martin (1985) used RWG and ML2.5 in simulations of North Pacific data. Both Martin and McCormick and Meadows used the same RWG model as written by Garwood and both generated nearly identical results with their idealized numerical experiments - the insignificant differences were expected because different equations of state were used in the two articles. This, therefore, provides a basis for extrapolating how ML2.5 may respond in large lakes based upon its performance under idealized conditions. Numerical experiments were conducted in both articles to isolate model response to idealized situations involving sustained heating, cooling and pure wind forcing. More detailed results can be found in those publications.

Under heating conditions the RT, RWG and ML2.5 models were similar to each other in their response by forming successively shallower ML depths with increased surface heat flux. The strong positive buoyancy flux generated by the heating retards mixing resulting in similar ML temperatures and depths among the models. Under strong cooling simulations the models behaved in a similar manner with each other. In this case the gravitational instabilities generated by surface cooling, and the simple adjustment mechanism used by the models to remove these instabilities, become the dominant feature controlling the ML temperature and depth. In general, both the strong heating and cooling regimes tend to mask model differences while wind-induced mixing highlights the greatest differences among the models.

Under deepening experiments the final ML depths as inferred from Martin (1985) and McCormick and Meadows (1988) suggest that the ML2.5 model would give the shallowest ML depth with RWG generating the deepest and RT falling in between the other two models. For example, under a 20 $m \cdot s^{-1}$ wind speed the final ML depth after 120 h of forcing would be 39 m for ML2.5 (Martin, 1985), 47 m for RT and 59 m for RWG (McCormick and Meadows, 1988). The rate of change of ML depth with respect

to wind stress, τ, is proportional to $\tau^{0.5}$ for each model. The changes in ML depths seen in this example are a potential concern for the modeler.

Although the ML depths may differ, their response time to storm conditions is rapid rendering them good candidates for applications where episodic events are important. Therefore, each of these models is potentially suitable for applications where rotational effects are important. For applications in smaller water bodies, however, the Dynamic Reservoir Simulation Model (DYRESM) (Imberger et al., 1978) is appropriate. Spigel and Imberger (1980) and Gorham and Boyce (1989) provide useful criteria for selecting a ML model based upon the relationship between ML dynamics and basin geometry.

3.4 CLIMATE CHANGE INFERENCES

Much effort has been spent and will continue to be spent studying all of the many facets involved with climate change. Relatively little is known about large lake climatology and subsequently even less about how future climate scenarios may impact any lake in question. McCormick (1990) used the RWG Model to investigate the sensitivity of a large lake (Lake Michigan) to three different climate change scenarios. The RWG Model was chosen because of its documented simulation skill and its ability to do long-term simulations without concern for an interannual carryover of potential energy that other models may induce (Garwood, 1977).

The three different climate change scenarios are described more fully in Chapter 2 (see Sections 2.6 - 2.8) and in other sources (e.g. see Mitchell, 1989) for a general review. Climate scenarios have been derived from the Goddard Institute for Space Studies (GISS), the Geophysical Fluid Dynamics Laboratory (GFDL), and the Oregon State University (OSU) Global Circulation Models (GCM's). Before these climate scenarios could be applied the base climatology had to be estimated. Because of the lack of long time-series of offshore temperature data the base climatology was estimated from model simulations from 1981 - 1984. This period corresponds to the most extensive offshore data set available.

Temperature data were obtained from NOAA's National Data Buoy Center (NDBC) buoy located in the center of the southern basin (42.7°N, 87.1°W) of Lake Michigan. The buoy is equipped with meteorological sensors and is deployed during the shipping season. During 1981 - 1984 the NDBC organizatioo attached a 50 m long thermistor string (total depth is approximately 150 m) to the buoy. Temperature sensors were spaced at 5 m intervals and recorded every hour. These data were supplemented with data collected by NOAA's Great Lakes Environmental Research Lab (GLERL) from nearby moorings from June 1982 to July 1984. The GLERL data provided temperature data at depth (50, 75 and 148 m).

Meteorological data used to run the model were obtained from two shoreline locations (Muskegon, Michigan and Milwaukee, Wisconsin) as well as from the NDBC buoy. The shoreline data was used primarily to supplement the NDBC buoy data during the winter months.

Results of the Base Climatology simulations resulted in an overall root mean squared error (RMSE) of 2.8°C (MeCormick, 1990). Additional simulations were performed with the wind speeds adjusted by ± 10% to quantify the impact of wind stress uncertainty on the simulations. When winds were lowered by 10% the overall RMSE improved to 2.3°C whereas a 10% increase in wind speed resulted in an increased RMSE of 3.5°C. These sensitivity studies demonstrated the dominant influence of wind speed on model results.

Once the Base Climatology was established the potential effects of climate change was estimated by calculating the ratio of double CO_2/single CO_2 for wind speed, air temperature, humidity, incident solar radiation at ground level, and fractional cloud cover. The doubled CO_2 input came from the monthly averaged output of GISS, GFDL and OSU and the single CO_2 input came from the baseline climatology used by these scenarios. After the ratio of double CO_2/single CO_2 was calculated the hourly meteorological input for the Lake Michigan simulation was altered by multiplying these data by the corresponding scenario ratio.

Figure 3-2 shows the simulation results from Base, GISS, GFDL, and OSU. The GISS, GFDL, and OSU simulations all showed increased surface water temperatures throughout the year. Both the GISS and GFDL simulations suggest the possibility of permanent stratification as seen by the absence of 4°C surface water. The OSU simulation, however, shows an annual overturn which occurs in early winter and persists until early spring.

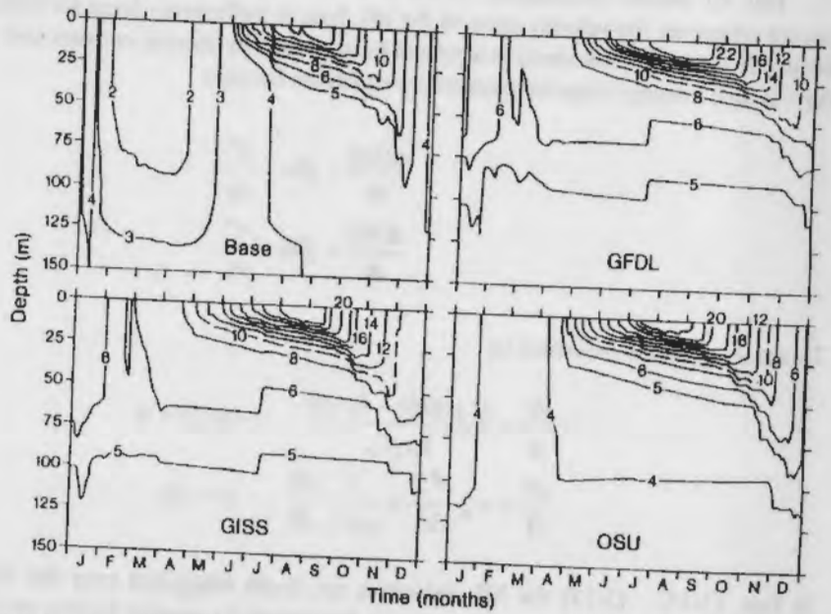

Figure 3-2. *Annual offshore temperature structure for Lake Michigan as inferred from Base climatology, and simulations based upon possible changes in climate as suggested by GFDL, GISS, and OSU scenarios.*

To better illustrate potential changes as suggested by these simulations the Base Climatology was subtracted from the GISS, GFDL, and OSU simulations (Figure 3-3). Figure 3-3 shows the changes in Lake Michigan's thermal structure. All of the scenarios suggest surface water temperature increases of up to 4°C and colder bottom temperatures during December. Although the OSU simulation does not show as much surface warming throughout the year as does GISS and GFDL it does show stronger summer stratification than those models. The OSU results also suggest colder bottom waters from April through December than seen in the Base Climatology. This colder than present changes in bottom temperatures result from both reduced vertical mixing due to stronger stratification and an increase in the duration of a stratified water column.

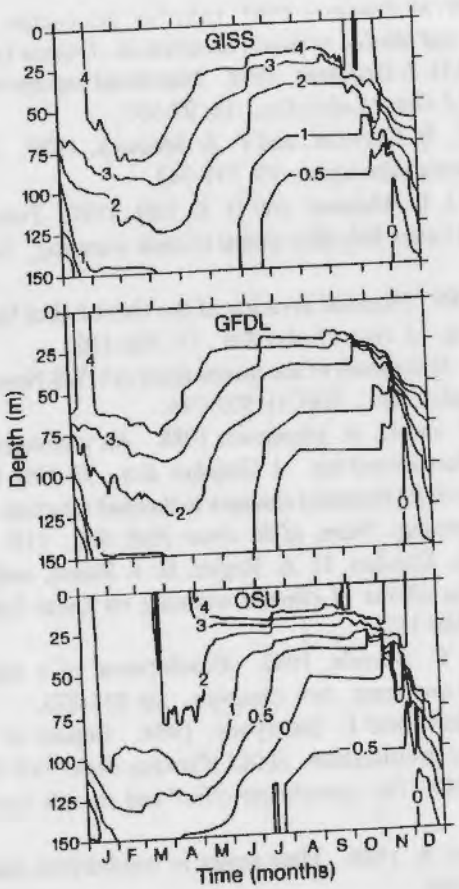

Figure 3-3. *Net changes to the annual offshore temperature structure of Lake Michigan under GFDL, GISS, and OSU scenarios. The Base climatology was subtracted from each of these simulations to better illustrates the differences.*

Serious reservations exist over any inference about changes to climatology and this Lake Michigan study is subject to the same concerns. McCormick (1990) describes in detail some of these reservations such as the use of monthly averaged data when in fact over 90% of the energy associated with ML deepening occurs at daily and higher frequencies (McCormick and Meadows, 1988). Therefore, this exercise is most useful for documenting the sensitivity of the system to changes in the monthly net surface heat flux. It is the temporal redistribution of the surface heat flux that is responsible for the simulated changes. The annual net surface heat flux change did not exceed 10 $W \bullet m^{-2}$ (Base vs GFDL) and if this change were uniformly distributed in time it would do little to explain the simulation results. Furthermore, if reliable scenario information were available at higher frequencies (daily) then even more dramatic changes may occur. Given all of the uncertainties surrounding estimates of future climate these results are best viewed as a sensitivity study wherein the scales selected for the sensitivity tests are based upon the different general circulation model scenarios.

The conclusions of this climate sensitivity study as applied to large deep lakes like Lake Michigan suggest the following possibilities. (1) Surface water temperatures would be higher throughout the year and bottom temperatures would be colder for at least one month (December). (2) The heat content would also be higher with the greatest increase in winter. However, after cold winters the following autumn heat content under OSU may actually decrease relative to present conditions. (3) The ML depth would be shallower in summer and the temperature gradients across the thermocline would be larger. Thus, more energy would be required to generate large scale vertical mixing. (4) The duration of the summer stratification period would be increased by up to 2 months with the biggest portion of the change occurring in an earlier springtime onset to stratification. (5) Under GISS and GFDL scenarios, the lake may no longer turnover fully during most winters. This may cause a permanent thermocline to form in deeper regions of the lake. If this occurs, and if these regions are polluted, then the consequent reduction in large scale vertical mixing suggests an increased potential for additional water quality degradation.

3.5 REFERENCES

Allender, J. H., and J. H. Saylor. 1979. Model and observed circulation throughout the annual temperature cycle of Lake Michigan. *J. Phys. Oceanogr.*, 9: 573-579.

Assel, R. A. (1991). Implications of CO_2 warming on Great Lakes ice cover. *Climatic Change*, 18: 377-395.

Assel, R. A., and F. H. Quinn. 1979. A historical perspective of the 1976-77 Lake Michigan ice cover. *Mon. Weather Rev.*, 107: 336-341.

Ayers, J. C. 1965. The climatology of Lake Michigan. *University of Michigan, Great Lakes Research Division*, Publication 12, 73p.

Ayers, J. C., D. C. Chandler, G. H. Lauff, C. F. Powers, and E. B. Henson. 1958. Currents and water masses of Lake Michigan. *University of Michigan, Great Lakes Research Division*, Publication 3, 169p.

Batchelor, G. K., and A. A. Townsend. 1956. Turbulent diffusion. Surveys in mechanics, G. K. Batchelor and R. M. Davies, eds., Cambridge University Press, New York, 352-399.

Bennett, J. R. 1977. A three-dimensional model of Lake Ontario's summer circulation. *J. Phys. Oceanogr.*, 7: 591-601.

Bennett, J. R. 1978. The circulation of large lakes. Upwelling ecosystems, R. Boje and M. Tomczak, eds., Springer-Verlag, Berlin, 223-234.

Blumberg, A. F., and D. M. DiToro. 1990. Effects of climate warming on dissolved oxygen concentrations in Lake Erie. *Trans. of the Amer. Fish. Soc.*, 119: 210-223.

Boyce, F. M. 1974. Some aspects of Great Lakes physics of importance to biological and chemical processes. *J. Fisheries Res. Board*, 31: 689-730.

Chen, C. T., and F. J. Millero. 1986. Precise thermodynamic properties for natural waters covering only the limnological range. *Limnol. Oceanogr.*, 31(3): 657-662.

Church, P. E. 1945. The annual temperature cycle of Lake Michigan. II. (Spring warming and summer stratification period 1942). *Department of Meteorology, University of Chicago*, MR 18, 100p.

Croley, T. E., II 1990. Laurentian Great Lakes double-CO_2 climatic change hydrological impacts. *Climatic Change*, 17: 27-47.

Csanady, G. T. 1972. The coastal boundary layer in Lake Ontario. Part I: The spring regime. *J. Phys. Oceanogr.*, 2: 41-53.

Csanady, G. T. 1975. Lateral momentum flux in boundary currents. *J. Phys. Oceanogr.*, 5: 705-717.

Cushman-Roisin, B. 1981. Deepening of the wind-mixed layer: A model of the vertical structure. *Tellus*, 33: 564-582.

Davis, R. E. 1983. Oceanic property transport, Lagrangian particle statistics, and their prediction. *J. Mar. Res.*, 41: 163-194.

Deardorff, J. W. 1970. A three-dimensional numerical investigation of the idealized planetary boundary layer. *Geophys. Fluid Dyn.*, 1: 377-410.

De Ruijter, W. P. M. 1983. Frontogenesis in an advective mixed-layer model. *J. Phys. Oceanogr.*, 13: 487-495.

De Szoeke, R. A. 1980. On the effects of horizontal variability of wind stress on the dynamics of the ocean mixed layer. *J. Phys. Oceanogr.*, 10: 1439-1454.

Garwood, R. W., Jr. 1977. An oceanic mixed layer capable of simulating cyclic states. *J. Phys. Oceanogr.*, 7: 455-468.

Gorham, E., and F. M. Boyce. 1989. Influence of lake surface area and depth upon thermal stratification and the depth of the summer thermocline. *J. Great Lakes Res.*, 15(2): 233-245.

Henderson-Sellers, B. 1985. New formulation of eddy diffusion thermocline models. *Appl. Math. Modelling*, 9: 441-446.

Henderson-Sellers, B. 1988. Sensitivity of thermal stratification models to changing boundary conditions. *Appl. Math. Modelling*, 12: 31-43.

Hill, D. K., and J. J. Magnuson 1990. Potential effects of global climate warming on the growth and prey consumption of Great Lakes fish. *Trans. of the Amer. Fish. Soc.*, 119: 265-275.

Hoeber, H. 1972. Eddy thermal conductivity in the upper 12m of the tropical Atlantic. *J. Phys. Oceanogr.*, 2: 303-304.

Ivanoff, A. 1977. Oceanic absorption of solar energy. Modelling and prediction of the upper layers of the ocean, E. B. Kraus, ed., Pergamon press, 47-72.

Imberger, J., J. Patterson, B. Hebbert, and I. Loh. 1978. Dynamics of reservoir of medium size. *ASCE J. Hydraul. Div.*, 104: 725-743.

Johnson, T. B., and D. O. Evans. 1990. Size-dependent winter mortality of young-of-the-year white perch: Climate warming and invasion of the Laurentian Great Lakes. *Trans. of the Amer. Fish. Soc.*, 119: 301-313.

Kraus, E. B., and J. S. Turner. 1967. A one-dimensional model of the seasonal thermocline, part II. *Tellus*, 19: 98-105.

Lam, D.C.L., and W. M. Schertzer. 1987. Lake Erie thermocline model results: comparison with 1967-1982 data and relation to anoxic occurrences. *J. Great Lakes Res.*, 13: 757-769.

Lesht, B. M., and D. J. Brandner. 1992. Functional representation of Great Lakes surface temperatures. *J. Great Lakes Res.*, 18: 98-107.

Magnuson, J. J., L. B. Crowder, and P. A. Medvick. 1979. Temperature as an ecological resource. *American Zoologist*, 19: 331-343.

Magnuson, J. J., J. D. Meisner, and D. K. Hill. 1990. Potential changes in the thermal habitat of Great Lakes fish after global climate warming. *Trans. of the Amer. Fish. Soc.*, 119: 254-264.

Mandrak, N. E. 1989. Potential invasion of the Great Lakes by fish species associated with climatic warming. *J. Great Lakes Res.*, 15: 306-316.

Martin, P. J. 1985. Simulation of the mixed layer at OWS November and Papa with several models. *J. Geophys. Res.*, 90(C1): 903-916.

McCormick, M. J., and G. A. Meadows. 1988. An intercomparison of four mixed layer models in a shallow inland sea. *J. Geophys. Res.*, 93 (C6): 6774-6788.

McCormick, M. J. 1990. Potential changes in thermal structure and cycle of Lake Michigan due to global warming. *Trans. of the Amer. Fish. Soc.*, 119: 183-194.

Meisner, J. D., J. L. Goodier, H. A. Regier, B. J. Shuter, and W. J. Christie. 1987. An assessment of the effects of climate warming on Great Lakes basin fishes. *J. Great Lakes Res.*, 13: 340-352.

Mellor, G. L., and T. Yamada. 1982. Development of a turbulence closure model for geophysical fluid problems. *Rev. Geophys.*, 20: 851-875.

Meyer, G., I. Masliev, and L. Somlyody. 1994. Impact of climate change on global sensitivity of lake stratification. *IIASA Working Paper* WP-94-28, 56p.

Mitchell, J. F. B. 1989. The 'greenhouse effect' and climate change. *Reviews of Geophys.*, 27: 115-139.

Mohammed-Zaki, M. A. 1980. Time scales in wind-driven lake conditions. *J. Geophys. Res.*, 85: 1553-1562.

Mortimer, C. H. 1974. Lake hydrodynamics. *Mitt. Intern. Ver. Limnol.*, 20: 124-197.

Müller, P., and R. W. Garwood Jr 1988. Mixed layer dynamics: Progress and new directions. *EOS*, 69(1): 2-4.

Munk, W. H., and E. R. Anderson. 1948. Notes on a theory of the thermocline. *J. Mar. Res.*, 7: 276-295.

Murthy, C. R., and D. S. Dunbar. 1981. Structure of the flow within the coastal boundary of the Great Lakes. *J. Phys. Oceanogr.*, 11: 1567-1577.

Niiler, P. P., and E. B. Kraus. 1977. One dimensional models of the upper ocean. Modelling and prediction of the upper layers of the ocean, E. B. Kraus, ed., Pergamon Press, 143-172.

Oort, A. H., and A. Taylor. 1969. On the kinetic energy spectrum near the ground. *Mon. Weather Rev.*, 97: 623-636.

Pollard, R. T., P. B. Rhines, and R. O. R. Y. Thompson. 1973. The deepening of the wind-mixed layer. *Geophys. Fluid Dyn.*, 3: 381-404.

Ramp, S. R., R. W. Garwood, C. O. Davis, and R. L. Snow. 1991. Surface heating and patchiness in the coastal ocean off Central California during a wind relaxation event. *J. Geophys. Res.*, 96(C8): 14947-14957.

Regier, H. A., J. A. Holmes, and D. Pauly. 1990. Influence of temperature changes on aquatic ecosystems: An interpretation of empirical data. *Trans. of the Amer. Fish. Soc.*, 119: 374-389.

Reynolds, O. 1894. On the dynamical theory of incompressible viscous fluids and the determination of the criterion. *Phil. Trans. Roy. Soc. A.*, 186: 123-164.

Roberts, P. H. 1961. Analytical theory of turbulent diffusion. *J. Fluid Mech.*, 11: 257-283.

Saylor, J. H., J. C, K, Huang, and R. O. Reid. 1980. Vortex modes in southern Lake Michigan. *J. Phys. Oceanogr.*, 10: 1814-1823.

Simons, T. J. 1976. Verification of numerical models of Lake Ontario. III. Long term heat transports. *J. Phys. Oceanogr.*, 6: 372-378.

Simons, T. J. 1980. Verification of seasonal stratification models. Final Report, Institute for Meteorology and Oceanography, University of Utrecht, The Netherlands.

Smith, J. B. 1991. The potential impacts of climate change on the Great Lakes. *Bull. of the Amer. Meteor. Soc.*, 72(1): 21-28.

Spigel, R. H., and J. Imberger. 1980. The classification of mixed-layer dynamics in lakes of small to medium size. *J. Phys. Oceanogr.*, 10: 1104-1121.

Stefan, H., and D. E. Ford. 1975. Temperature dynamics in dimictic lakes. *Proc. ASCE J. Hyd. Div.*, 101: 97-114.

Taylor, G. I. 1931. Effect of variation in density on the stability of superposed streams of fluid. *Proc. Roy. Soc. London Ser. A.*, 132: 499-523.

Thompson, R. O. R. Y. 1976. Climatological numerical models of the surface mixed layer of the ocean. *J. Phys. Oceanogr.*, 6: 496-503.

Thompson, R. O. R. Y. 1979. A reinterpretation of the entrainment process in some laboratory experiments. *Dyn. Atmos. Oceans*, 4: 45-55.

Walters, R.T., G. F. Carey, and D. F. Winter. 1978. Temperature computation for temperate lakes. *Appl. Math. Modelling*, 2: 41-48.

Woods, J. D. 1977. Parameterization of unresolved motions. Modeling and prediction of the upper layers of the ocean, E. B. Kraus, ed., Pergamon press, Elmsford, New York, 118-142.

3.6 APPENDIX - BASIC THEORY

All of the mixed layer models are based in one way or another upon the governing conservation equations of mass, momentum, heat, and turbulence kinetic energy. Let $V = \overline{V} + v'$ where, V is a velocity vector with components (u,v,w) corresponding to a (x,y,z) coordinate system with x positive easterly, y positive northerly, and z positive from the surface upwards. $\overline{V}$ is the "mean" velocity and v' is the fluctuating component (u',v',w') and by definition $\overline{v'} = 0$, and $\overline{v'c} = 0$ where c is a constant. The overbar is a probability average or ensemble average but in practice it is approximated by some suitable time average. To avoid ambiguity it is referred to as Reynolds averaging after Reynolds (1894) who first introduced the concept. Applying this convention the conservation of mass equations can be written as

$$\nabla \bullet \overline{V} = 0 \qquad \text{(A3-1)}$$

$$\nabla \bullet v' = 0 \qquad \text{(A3-2)}$$

where $\nabla = (\frac{\partial}{\partial x}\vec{i} + \frac{\partial}{\partial y}\vec{j} + \frac{\partial}{\partial z}\vec{k})$ the gradient operator.

The conservation of momentum is expressed by the Navier - Stokes equations for an incompressible fluid,

$$\frac{\partial V}{\partial t} + V \bullet \nabla V + 2\Omega\vec{k} \times V = -g\vec{k} - \frac{1}{\rho}\nabla P + \upsilon\nabla^2 V \qquad \text{(A3-3)}$$

where,

Ω	$= \Omega_0 \sin(\theta)$
Ω_0	the angular velocity of the earth
θ	latitude
$\vec{k}$	unit vector positive upwards along vertical
x	vector cross product
ρ	water density
P	pressure
v	kinematic viscosity (μ/ρ), μ = molecular viscosity
∇^2	$(\frac{\partial^2}{\partial x^2}\vec{i} + \frac{\partial^2}{\partial y^2}\vec{j} + \frac{\partial^2}{\partial z^2}\vec{k})$ the Laplacian operator and
g	gravity.

The first two terms on the left hand side (LHS) of Eq. (A3-3) are the local time rate of change of momentum and the rate of change of momentum seen following the motion, respectively, and the final term on the LHS is due to the Coriolis effect. On the RHS of Eq. (A3-3) the first term is the gravitational force, the second is the pressure gradient force, and the last term is the viscous force. The equation of motion in the vertical can be reasonably approximated by the hydrostatic equation,

$$\frac{\partial P_0}{\partial z} = -\rho_0 g \qquad \text{(A3-4)}$$

because the vertical acceleration of fluid particles is small compared to g. If the Boussinesq approximation is made, i.e., density variations are unimportant with respect to all terms except those involving buoyancy, and Eq. (A3-4) is added to Eq. (A3-3) then

$$\frac{\partial V}{\partial t} + V \bullet \nabla V + 2\Omega \bar{k} \times V = -\frac{(\rho - \rho_0)}{\rho_0} g\bar{k} - \frac{1}{\rho_0}\nabla(P - P_0) + \upsilon \nabla^2 V . \qquad \text{(A3-5)}$$

Let $\rho_d = \rho - \rho_0$ and $P_d = P - P_0$ be the difference between the actual density and pressure minus the reference density and hydrostatic pressure, respectively. The resulting gravitational and pressure gradient terms are interpreted as the buoyancy and pressure forces due to dynamical conditions so that Eq. (A3-5) becomes

$$\frac{\partial V}{\partial t} + V \bullet \nabla V + 2\Omega \bar{k} \times V = -\frac{\rho_d}{\rho_0} g\bar{k} - \frac{1}{\rho_0}\nabla P_d + \upsilon \nabla^2 V . \qquad \text{(A3-6)}$$

Equation (A3-6) is the basis for deriving the mean turbulence equations of motion. The derivation begins by separating the density, pressure, and velocity variables into a mean and fluctuating component: $\rho_d = \bar{\rho}_d + \rho_d'$, $P_d = \bar{P}_d + P_d'$, and with the velocity decomposition already described they are then substituted into Eq. (A3-6) yielding

$$\frac{\partial(\bar{V} + v')}{\partial t} + (\bar{V} + v') \bullet \nabla(\bar{V} + v') + 2\Omega \bar{k} \times (\bar{V} + v') = \\ -\frac{(\bar{\rho}_d + \rho_d')}{\rho_0} g\bar{k} - \frac{1}{\rho_0}\nabla(\bar{P}_d + P_d') + \upsilon \nabla^2(\bar{V} + v') . \qquad \text{(A3-7)}$$

After Reynolds averaging Eq. (A3-7) and substituting the mass conservation equations we get the mean momentum equations

$$\frac{\partial \bar{V}}{\partial t} + \bar{V} \bullet \nabla \bar{V} + (\nabla \bullet \overline{v'v'}) + 2\Omega \bar{k} \times \bar{V} = -\frac{\bar{\rho}_d}{\rho_0} g\bar{k} - \frac{1}{\rho_0}\nabla \bar{P}_d + \upsilon \nabla^2 \bar{V} . \qquad \text{(A3-8)}$$

The Reynolds decomposition and averaging of the velocity is responsible for an additional momentum source (or sink) in Eq. (A3-8) compared to Eq. (A3-6). This is the third term on the LHS and is the contributioo to the mean momentum from the divergence of the turbulence velocity interactions or Reynolds stresses. Finally, the equations for the turbulence components of momentum transport are obtained by subtracting Eq. (A3-8) from Eq. (A3-7)

$$\frac{\partial v'}{\partial t} + \bar{V} \bullet \nabla v' + v' \bullet \nabla \bar{V} + v' \bullet \nabla v' - (\nabla \bullet \overline{v'v'}) + 2\Omega \bar{k} \times v' = \\ -\frac{\rho_d'}{\rho_0} g\bar{k} - \frac{1}{\rho_0}\nabla P_d' + \upsilon \nabla^2 v' . \qquad \text{(A3-9)}$$

Two remaining processes to be described are the conservation of thermal and turbulence kinetic energy. Conservation of thermal energy can be written as

$$\frac{\partial T}{\partial t} + V \bullet \nabla T = M_T \nabla^2 T + \frac{1}{\rho_0 C_P}\nabla \bullet R \qquad \text{(A3-10)}$$

where, T = temperature, M_T = molecular thermal diffusivity, C_p = specific heat at constant pressure, and R = penetrative component of solar energy, positive in the negative z direction. If Eq. (A3-10) is treated in a manner analogous to the previous equations with $T = \bar{T} + T'$, $R = \bar{R} + R'$, then the Reynolds averaged heat equation is

$$\frac{\partial \bar{T}}{\partial t} + \bar{V} \bullet \nabla \bar{T} + (\nabla \bullet \overline{v'T'}) = M_T \nabla^2 \bar{T} + \frac{1}{\rho_0 C_P}\nabla \bullet \bar{R} . \qquad \text{(A3-11)}$$

In the upper regions of the water column turbulence transport will generally dominate over molecular so that the first term on the RHS of Eq. (3-11) may be ignored producing

$$\frac{\partial \bar{T}}{\partial t} + \bar{V} \bullet \nabla \bar{T} = -(\nabla \bullet \overline{v'T'}) + \frac{1}{\rho_0 C_P}\nabla \bullet \bar{R} . \qquad \text{(A3-12)}$$

Finally, the turbulence kinetic energy (TKE) equations are derived by scalar multiplying Eq. (A3-9) by v' and then Reynolds averaging the result

$$\frac{\partial \bar{q}}{\partial t} + \bar{V} \bullet \nabla \bar{q} = -\frac{\overline{w'\rho_d'}}{\rho_0} g\bar{k} - \overline{v'(v' \bullet \nabla \bar{V})} - \nabla \bullet \overline{(v'q + \frac{v'P_d}{\rho_0})} + \upsilon \overline{v' \bullet \nabla^2 v'} \\ \bar{q} = \frac{1}{2}\overline{(u'u' + v'v' + w'w')} \qquad \text{(A3-13)}$$

The first term on the RHS of Eq. (A3-13) is the rate of TKE increases due to the work of buoyancy forces. For fresh water applications the density perturbations result from temperature fluctuations, hence it is referred as the thermal energy production term. The next term represents the mechanical energy production. The production rate is determined by the rate of energy transfer from the mean motion through turbulent shear stresses. The third term expresses the redistribution of the total turbulent energy by the divergence of the turbulent advection and pressure-work, respectively. And the last term signifies the rate of energy loss from the TKE by viscosity. In practice this term is approximated by -ε, the dissipation rate per unit mass of the turbulence into internal heat.

Equations (A3-1), (A3-8), (A3-12), and (A3-13) with the appropriate boundary conditions are sufficient to describe the evolution of the mean temperature field. However, these equations are highly nonlinear and fully three-dimensional requiring additional assumptions in order to make their solution tractable. For one-dimensional applications we assume that variations in temperature, velocity, and heat fluxes are small enough in the horizontal relative to the vertical that horizontal homogeneity can be assumed. Therefore, the one-dimensional modeling framework, with overbars omitted from the mean variables for notational convenience, is described by the following system of equations:

mass conservation

$$\frac{\partial u}{\partial x}+\frac{\partial v}{\partial y}+\frac{\partial w}{\partial z}=0 \qquad \text{(A3- 14)}$$

momentum

$$\frac{\partial u}{\partial t}-fv=\frac{1}{\rho_0}\frac{\partial \tau^x}{\partial z}$$

$$\frac{\partial v}{\partial t}+fu=\frac{1}{\rho_0}\frac{\partial \tau^y}{\partial z} \qquad \text{(A3-15)}$$

thermal energy

$$\frac{\partial T}{\partial t}=-\frac{\partial(\overline{w'T'})}{\partial z}+\frac{1}{\rho_0 C_p}\frac{\partial R}{\partial z} \qquad \text{(A3-16)}$$

turbulence kinetic energy

$$\frac{\partial q}{\partial t}=-\frac{\overline{w'\rho'}}{\rho_0}g\bar{k}+\frac{\tau^x}{\rho_0}\frac{\partial u}{\partial z}+\frac{\tau^y}{\rho_0}\frac{\partial v}{\partial z}-\frac{\partial}{\partial z}\left(\overline{w'q+\frac{w'P'}{\rho_0}}\right)-\varepsilon \qquad \text{(A3-17)}$$

where, $f=2\Omega_0\sin(\theta)$, and the surface shear stresses in the x and y directions, respectively, are: $\tau^x=-\rho_0\overline{u'w'}$, $\tau^y=-\rho_0\overline{v'w'}$.